Available online at www.sciencedirect.com
ScienceDirect
Journal of Bionic Engineering 11 (2014) 600–609

Biomimetic Collagen/Hydroxyapatite Composite Scaffolds: Fabrication and Characterizations

Jiancang Wang[1], Chaozong Liu[2]

1. *Department of Ophthalmology*, *Children's Hospital of Hebei Province*, *Shijiazhuang* 050031, *P. R. China*
2. *John Scales Centre for Biomedical Engineering*, *Institute of Orthopaedics and Musculoskeletal Science*, *University College London*, *Royal National Orthopaedic Hospital*, *Stanmore*, *London HA*7 4*LP*, *UK*

Abstract

Biomimetic collagen/hydroxyapatite scaffolds have been prepared by microwave assisted co-titration of phosphorous acid-containing collagen solution and calcium hydroxide-containing solution. The resultant scaffolds have been characterised with respect to their mechanical properties, composition and microstructures. It was observed that the *in situ* precipitation process could combine collagen fibril formation and hydroxyapatite (HAp) formation in one process step. Collagen fibrils guided hydroxyapatite precipitation to form bone-mimic collagen/hydroxyapatite composite containing both intrafibrillar and interfibrillar hydroxyapatites. The mineral phase was determined as low crystalline calcium-deficient hydroxyapatite with calcium to phosphorus ratio (Ca/P) of 1.4. The obtained 1% (collagen/HAp = 75/25) scaffold has a porosity of 72% and a mean pore size of 69.4 μm. The incorporation of hydroxyapatite into collagen matrix improved the mechanical modulus of the scaffold significantly. This could be attributed to hydroxyapatite crystallites in collagen fibrils which restricted the deformation of the collagen fibril network, and the load transfer of the collagen to the higher modulus mineral component of the composite.

Keywords: scaffold, bone tissue engineering, collagen, hydroxyapatite, biomimetic

doi: 10.1016/S1672-6529(14)60071-8

1 Introduction

Bone is a hierarchically structured inorganic-organic composite material consisting of hydroxyapatite nanorods embedded in a collagen matrix. It contains 60%–70% mineral component in the form of small apatite crystals, 20%–30% collagen fibers, and 10%–20% water[1]. The mineral component of the bone is composed mainly of carbonated apatite with low crystallinity. The main constituent of the mineral component is hydroxyapatite with the chemical formula $Ca_{10}(PO_4)_6(OH)_2$) which has a Ca/P ratio of 1.67. Collagen is the main fibrous protein in the body and a significant constituent of the natural extracellular matrix. Collagen has a triple helical structure, and specific points along the collagen fibrils serve as nucleation sites for the bone mineral crystals. The collagen fibrils guide the precipitation and growth of nano-apatite crystals to form a nano-structured architecture consists of uniaxially oriented nano-HAp crystals embedded in collagen matrix and aligned parallel to the long collagen fibril axes[2]. Its unique molecular structure, microstructure and macrostructure give bone the unique mechanical properties to withstand dynamic loading.

Both collagen and hydroxyapatite have been used in bone tissue engineering owing to their excellent osteoconductive property. The composite scaffold of these two natural materials has been proved to be more useful than a monolithic one. The ductile property of collagen increases the fracture toughness and decreases the stiffness of hydroxyapatite. While the addition of hydroxyapatite to collagen matrix improves the mechanical stability of the scaffold in both dry and wet conditions[3,4], and accelerates osteogenesis[5]. Furthermore, by integrating rapid fabrication technology, *in situ* precipitation and mutil-layer stacking processing method, the structure and composition of collagen and hydroxyapatite nanocomposite could be manipulated to

Corresponding author: Chaozong Liu
E-mail: Chaozong.Liu@ucl.ac.uk

make functionally gradient scaffold to mimick and replace skeletal bone[6–8].

Bone substitutes, generated by a tissue engineering approach, allow repair mechanisms to take place by providing a temporary porous scaffold that reduces the size of the defect which needs to be repaired. The scaffold provides a mechanical support to the cells until the tissue has regenerated and remodeled itself naturally. In this application, the scaffold can be seeded with specific cells and signaling molecules in order to maximize tissue growth, and the rate of degradation and absorption of these scaffold materials can be controlled[6]. Well defined and controlled architecture, which can facilitate cellular infiltration and transport of nutrients and waste products, are essential[9–11]. The rationale behind mimicking the organization of the bone in a single scaffold is to create an environment that more closely resembles the natural Extra Cellular Matrix (ECM) of bone[12]. The most direct approach to provide "bioactive" bone-like material is to create a "mimic" composition, nanostructure and biological response that is similar to the bone. Many researchers have developed processing routes to prepare biomimetic collagen/HAp composite with respect to morphology, structure and mineralisation[13–15]. In practice, direct mineralisation of collagen involves collagen fibril mediated precipitation of nanohydroxyapatite from the reaction of calcium-containing and phosphate-containing solutions[13,16].

In this work, biomimetic collagen/hydroxyapatite composite 3D porous scaffolds have been fabricated by using a microwave-assisted *in situ* collagen mineralization process. In this method, a phosphoric acid-containing collagen solution and a calcium-containing solution are simultaneously added into a reaction vessel through a pump at a predefined rate and controlled condition (pH=9, and temperature at 40 ˚C). The co-precipitation process allows self-organization of hydroxyapatite and collagen. The parameters which influence the formation and the nano-structure of nano-hydroxyapatite crystallites have been examined, and the resultant scaffolds have been investigated with respect to their morphology, microstructure and dynamic mechanical properties. The obtained results would provide useful information for the collagen-hydroxyapatite scaffolds to produce physical microenvironment for the cells growth and tissue formation.

2 Materials and methods

2.1 Preparation of bone-mimetic collagen/HAp composite

The collagen/HAp composite was fabricated using a modified *in situ* collagen mineralization method that has been previously described[17]. The modified method uses a microwave reactor to assist the collagen mineralization process, the experiment setup is shown in Fig. 1. The *in situ* mineralization of collagen was based on the solution reaction of calcium hydroxide and phosphoric acid (Sigma-Aldrich, UK) in the present of collagen. The collagen dispersion was produced from microfibrillar type 1 collagen isolated from bovine Achilles tendon (Sigma-Aldrich, UK). To make collagen/hydroxyapatite nanocomposite, the phosphate-containing collagen dispersion (0.5% (w/v) collagen dispersion contains 0.3 mM H_3PO_4) was co-titrated with 0.5 mM $Ca(OH)_2$ solution at the rate of 1 mL per minute by using a high-end titrator (Metrohm

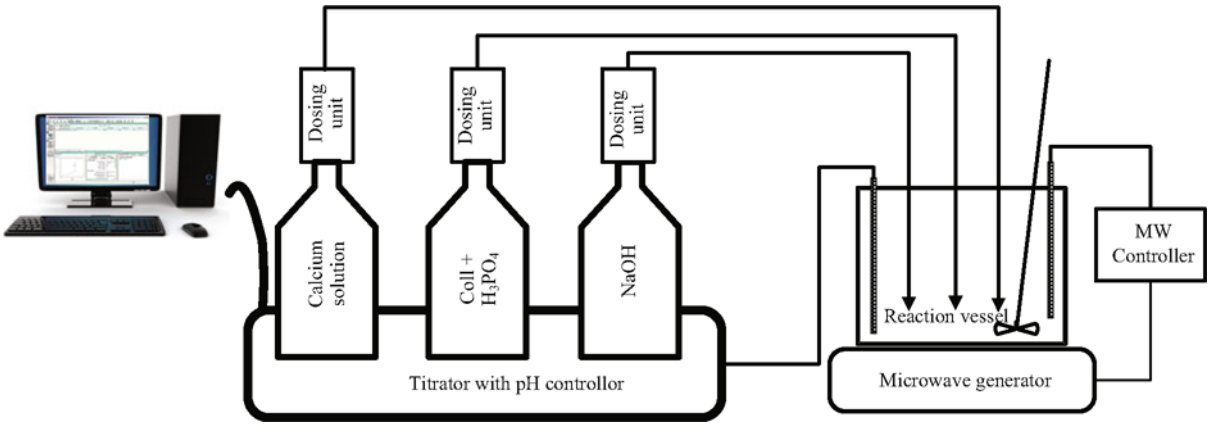

Fig. 1 Schematic of the experimental setup for *in situ* collagen/HAp composite preparation.

907, Metrohm Ltd. UK). The amounts of $Ca(OH)_2$ and H_3PO_4 were determined based on the stoichiometric Ca/P molar ratio of 1.67 for hydroxyapatite. The titrator has three dosing units (Fig. 1): one is used to deliver collagen-H_3PO_4 aqueous solution, second to deliver $Ca(OH)_2$ solution and third to deliver Na(OH) solution in order to maintain the pH value during *in situ* mineralization process. The reaction was performed in a START SYNTH microwave reactor (Milestone Inc, USA) with temperature maintained at 90 ˚C through a temperature control unit.

After the reaction, the suspension was incubated for 5 days at 37 ˚C, then degased and centrifuged to obtain collagen/HAp composite. The collagen/HAp composite scaffolds were fabricated by casting the composite suspension into a polytetrafluoroethylene (PTFE) mould and freezing at −20 ˚C for 24 hours, then, freeze drying to obtain the porous scaffolds.

2.2 Characterisations of the composites

The microstructure of the composite and scaffold were examined by Scanning Electron Microscopy (SEM) (JEOL JSM-840F, JEOL) operated at an accelerating voltage of 5 kV, after sputter deposition of a conductive platinum film (2 nm). The pore size and size distribution of the samples were analyzed by a high resolution micro X-ray computed tomography (micro-CT) system (CT 40, Scanco Medical, Switzerland) operated at a voltage of 55 kV and a current of 145 mA. Samples were scanned at 8 μm volume pixel (voxel) resolution with an integration time of 300 ms to produce 3D reconstructed images. After titration, the dispersed collagen/HAp composite in water was scooped on a cupper mesh with a carbon membrane for Transmission Electro Micrography (TEM) examinations. The obtained TEM specimens were examined by TEM (LEM-200CX, JEOL) in bright field model to assess the mineral phase morphology and interaction between collagen fibrils and the mineral phase. Electron diffraction patterns of the crystallites were used to identify the calcium phosphate phase. The local elemental analysis was carried out by a fitted EDAX Genesis system to assist the phase identification.

The mineral phase was investigated by a multipurpose diffractometer ((XPERT PRO MRD, PANalytical) operated at 40 kV and 40 mA using Cu radiation (λ=0.15418 nm) over a 2θ range from 5˚ to 70˚ at increment of 0.001˚. 1 mg specimen was mixed with potassium bromide (KBr) powder and ground using an agate mortar and pestle. The resulting mixture was pressed into transparent disc with a diameter of 13 mm. Fourier Transform Infra-red (FTIR) spectra of the sample was examined in transmission mode using FTIR spectrometer (Spectrum 2000, Perkin Elmer) from the specimen disc in the range from 4000 cm^{-1} to 400 cm^{-1} at a resolution of 4 cm^{-1}.

Surface chemistry of the samples was determined using a K-Alpha X-ray Photoelectron Spectroscopy (XPS) system (Thermo Scientific, UK). The X-ray source used was Mg Kα line ($h\nu$=1253.6 eV), operating at an emission voltage and current of 20 mA. A survey scan in the range from 0 eV to 1000 eV was performed and high resolution spectra were also obtained.

Dynamic mechanical properties of the scaffolds were analyzed using a dynamic mechanical analyzer (DMA8000, PerkinElmer, UK). The dynamic tests on compression, tensile and shear modes were performed on scaffolds in wet condition at 37 ˚C. The sample was loaded into a sample holder, then dynamic stress was applied to the sample to a displacement of 0.5 mm at frequency of 1 Hz. The changes in strain, phase angle, tanδ and modulus, that related to the viscoelastic behaviour of the scaffolds, were monitored during the test.

3 Results

3.1 Microstructure of the scaffolds

The properties of the obtained biomimetic collagen/HAp scaffolds are dependent on the mineral size, composition and the *in situ* conditions for hydroxyapatite formation. In this study, the final volume of the collagen/HAp dispersion was adjusted to 100 mL by water evaporation. The collagen concentration in the final dispersion is equivalent to 1%, with a collagen/HAp mass ratio of 75/25. The obtained composite scaffold demonstrated an interconnected pore network, as revealed by micro-CT examination in Fig. 2a. It was observed that the resultant nanocomposites have a broad range of pore sizes ranging from less than 20 μm to larger than 300 μm. Detailed analysis indicated that the obtained scaffold has a porosity of 72% and a mean pore size of 69.4 μm, as shown in Fig. 2b.

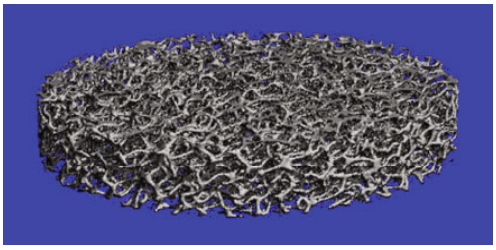

(a)

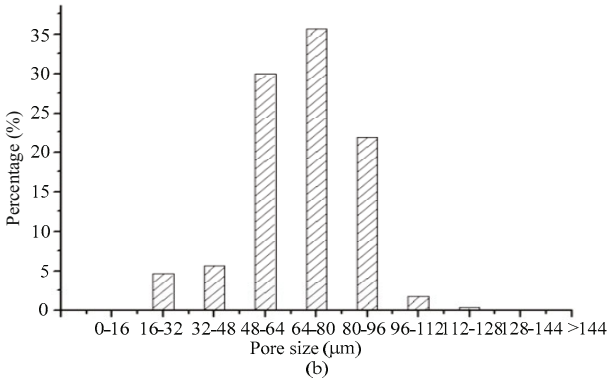

(b)

Fig. 2 (a) Micro-CT examination: 1% m/v scaffold with collagen/HAp ratio of 75/25, porosity of 72% and mean pore size of 69.44±17.6 μm. (b) pore size distribution within scaffold.

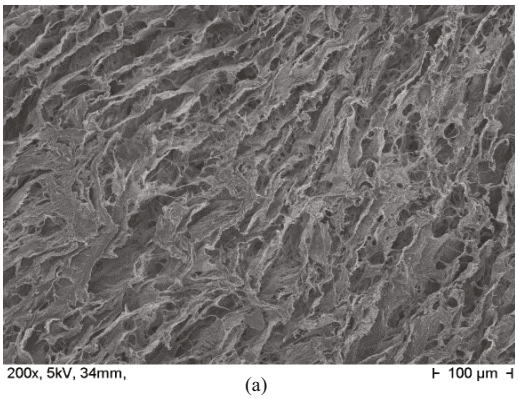

(a)

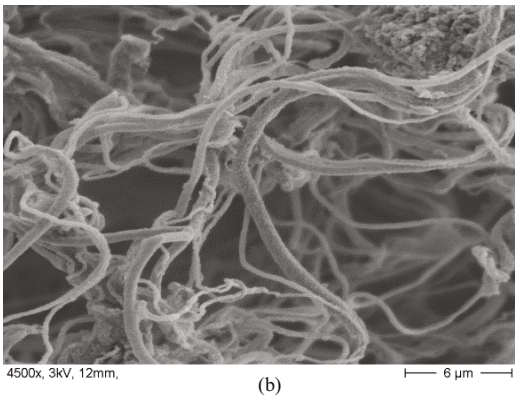

(b)

Fig. 3 SEM micrograph of collagen/HAp composite scaffold. (a) The oriented micro-channels (low magnification); (b) the interfibrillar hydroxyapatite clusters .

It is well established that the pore size and porosity of the scaffold play a critical role in cell ingrowth and cell growth. The pores need to be large enough to allow cells to migrate into the structure, but small enough to establish a sufficiently high specific surface for a minimal ligand density required for efficient binding of a critical number of cells to the scaffold[18]. It is generally accepted that the optimal pore size is different for each specific cell type and tissue product. In the case of collagen/HAp composite, the pore size and porosity could be controlled in final collagen concentration and freezing rate. Generally speaking, the lower concentration produces larger pores than that of the higher concentration dispersion, and slower freezing rate results in bigger pores than that of fast freezing rate, as reported elsewhere[19,20].

Fig. 3a shows the SEM image of the cross-sectional area of collagen/HAp composite. This image illustrates that micro-channels exist in the scaffold. These micro-channels align longitudinally, and parallel to the direction of solidification, i.e. heat transfer direction. The formation of such longitudinally oriented micro-channel networks could be explained by a planar ice front growth theory as described elsewhere[21]. The pores within scaffold arise from the ice crystals, which formed during the freezing of collagen dispersion. This forces collagen to aggregate into the interstitial spaces and create an interconnected network of collagen fibrils, as shown in Fig. 3b. The ice crystals grow to the vertical direction excluding the collagen/HAp nanocomposite in solidification. After sublimation of ice crystals, the spaces occupied by the ice crystals become pores, and result in a unidirectionally interconnected pore network. The size of the channels and the spacing between them range from several microns to 100 microns. A previous study has reported the pore size of the scaffold could be adjusted by altering the concentration of collagen dispersion and the addition of hydroxyapatite, the freezing rate and the pH value since these factors are known to affect both the nucleation and growth rates of ice crystals[22]. Higher collagen concentration and higher freezing rate of the dispersion produce a lower porosity and smaller pore sizes; while higher porosity and larger pore size scaffolds could be obtained by lowing collagen concentration and freezing rate[23].

Detailed examination of collagen fibril networks revealed that collagen fibrils influence the precipitation

process of hydroxyapatite, as shown in Fig. 3b. This image illustrates some nano-hydroxyapatite covering the collagen fibrils, and some nanohydroxyapatite clusters filling part of the voids of the composite.

3.2 Mineral phase and mineralisation of collagen matrix

XRD was used to examine the mineral phase of the composite, and commercially available hydroxyapatite powder (Sigma-Aldrich, UK) was used as control. The XRD spectra of the control sample and the obtained composite are shown in Fig. 4. The phase composition of the precipitated nano-crystallite was identified as hydroxyapatite of low crystallinity. The two main peaks in the XRD spectra correspond to d-spacings of 2.816 Å and 3.45 Å, respectively. The strongest (211) peak at 31.9° corresponds to hydroxyapatite (P63/m) belonging to the hexagonal symmetry. These values are in agreement with the JCPDS 9-432 card of hydroxyapatite.

The electron diffraction pattern of the specimen is shown in Fig. 5. It exhibits a large number of typical rings of a low crystalline structure. From the rings corresponding to the basal planes (002) and (300), the lattice parameters, a and c, can be determined as a = 0.943 nm and c = 0.689 nm, respectively. As seen from the TEM bright field image, electron-dense swollen collagen fibrils with regular cross-bands could be identified. Low magnification TEM (Fig. 5a) revealed that the collagen fibrils guide the precipitation of hydroxyapatite, and hydroxyapatite clusters were deposited onto the collagen fibrils, confirmed by the high magnification TEM analysis (Fig. 5b) revealing the heavily mineralized fibrils. The thin plate-like nano-hydroxyapatite platelets precipitated inside the collagen fibrils to form collagen-hydroxyapatite composite. These intrafibrillar nano-hydroxyapatite crystallites were 10 nm – 30 nm long along their c-axes and were responsible for the cross-banded appearance of the mineralized collagen fibrils. The c-axes of hydroxyapatite crystallites are aligned with the elongation of the collagen fibrils. The

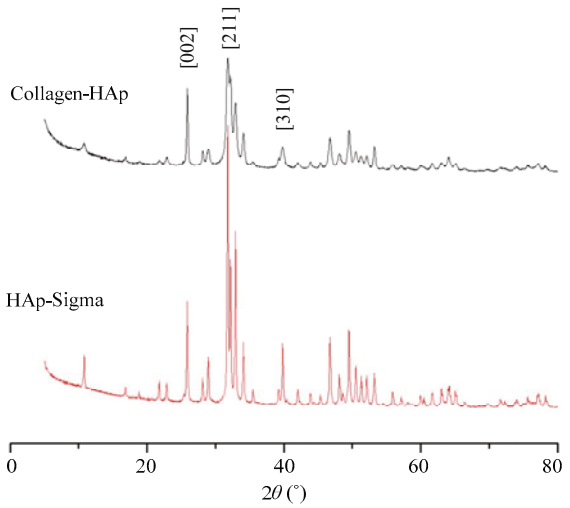

Fig. 4 XRD analysis of biomimetic collagen/HAp (75/25) composite and hydroxpapatite powder.

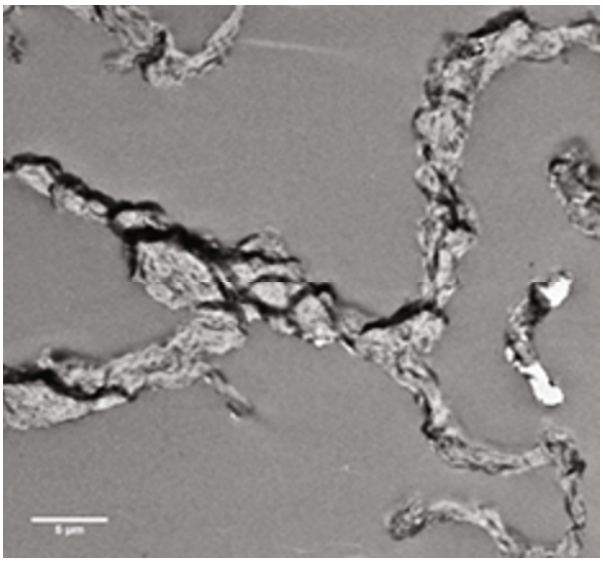

(a)

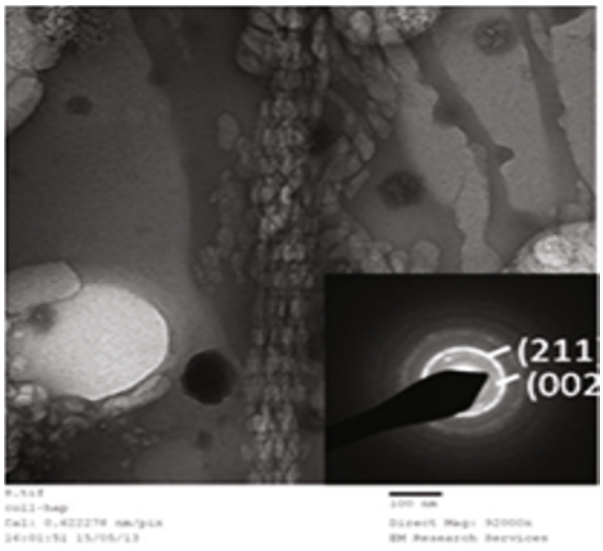

(b)

Fig. 5 The electron diffraction pattern of biomimetic collagen/HAp (75/25) composite. (a) collagen fibrils guided nano-HAp precipitatation, which deposits onto collage fibrils to form interfibrillar hydroxyapatite agglomerates; (2) HAp nanocrystallites precipitating inside collagen fibril to form intrafibrillar hydroxyapatite.

architecture of collagen/Hap nanocomposite is similar to those found in mammalian bone[24,25] and in mineralized collagen fibril of human bone tissue[26]. These intrafibrillar nano-hydroxyapatite crystallites protect the collagen fibrils from dehydration shrinkage.

The chemical composition of the collagen/HAp composite was evaluated more specifically using FTIR spectroscopy. The spectra of collagen and composite scaffolds are shown in Fig. 6. For collagen scaffold, the spectrum exhibited typical amide bands derived from collagen. The peak at 1650 cm^{-1} is assigned to amide I arised from the C=O stretch of the collagen, and the peaks at 1550 cm^{-1} and 1235 cm^{-1} are assigned to amide II and amide III, derived from the N-H in plane deformation plus C-N stretch of collagen, respectively[27]. Normally, the amide I band is strong, the amide II band is weak and the amide III is moderate. The typical bands, such as N-H stretching at 3330 cm^{-1} for the amide A and C-H stretching at 3070 cm^{-1}, are also evidenced in the spectrum[12,23,28]. For collagen/HAp composite scaffold, in addition to the main peaks of collagen namely amide I, II and III, the spectrum also exhibited bands derived from hydroxyapitate, which formed main peaks of the spectrum. A broad phosphate band in the range from 1150 cm^{-1} to 950 cm^{-1} arises from the P-O asymmetric stretching mode ($v3$) of the phosphate groups. The triple ($v4$) degenerate bending modes of O-P-O bond were exhibited at 600 cm^{-1} and 570 cm^{-1}[29,30].

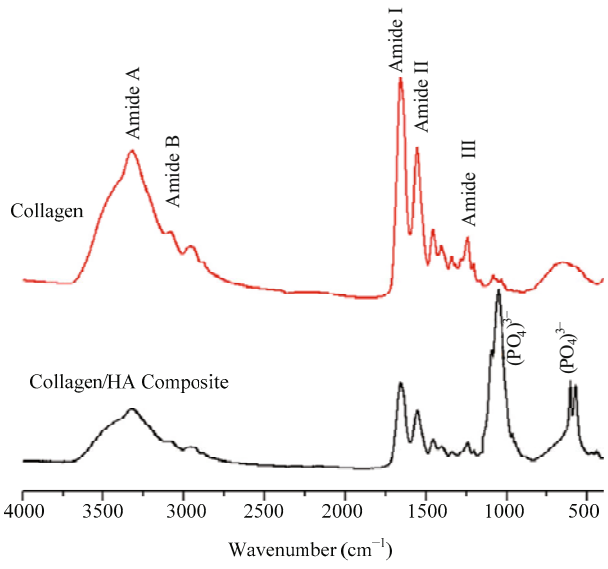

Fig. 6 FTIR spectra of collagen and collagen/HAp composite.

3.3 Mechanical property

To determine the influence of addition of hydroxyapatite on the dynamic property of the composite, dynamic mechanical tests were performed on composite samples with varied collagen/HAp ratio. Fig. 7 reports the dynamic modulus variations with collagen/HAp ratio (by mass). It was observed that all three moduli

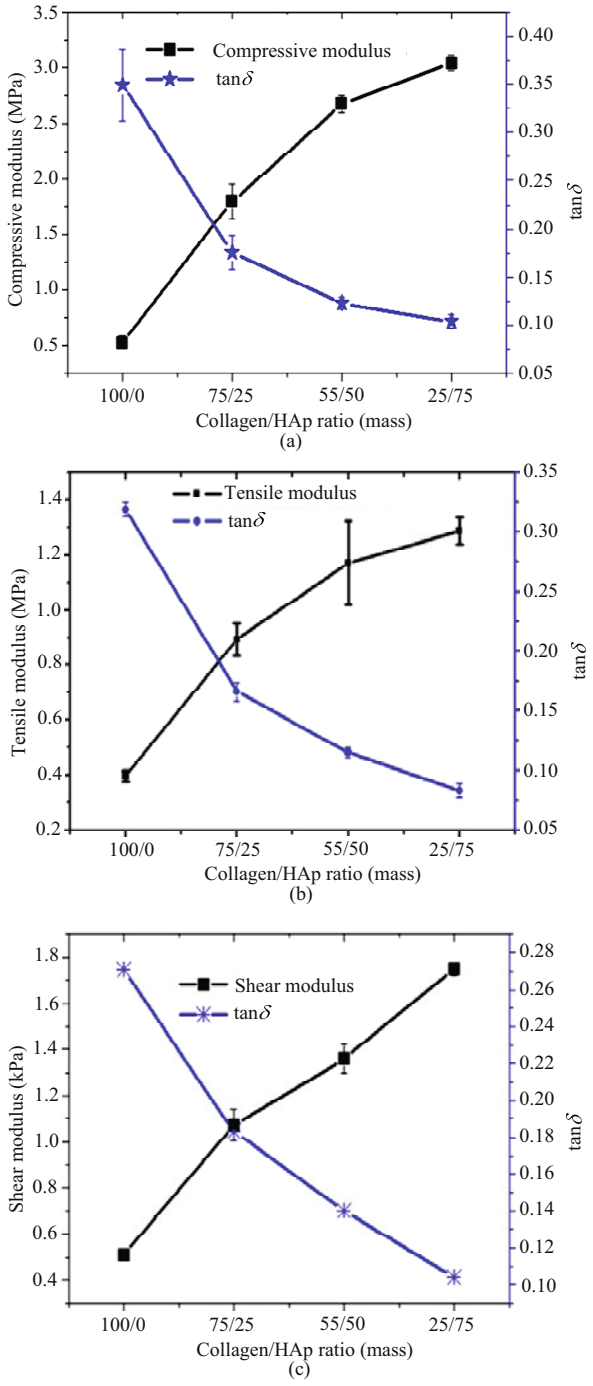

Fig. 7 Mechanical properties of collagen/HAp composite as determined by Dynamic Mechanical Analyser (DMA). (a) compressive modulus and tanδ; (b) tensile modulus and tanδ; and (c) shear modulus and tanδ.

(compressive, tensile and shear) of the scaffold increased with the collagen/HAp ratio. The pure collagen scaffold has a compressive modulus of 0.5 MPa, while the composite scaffold, which contains 75% of HAp, has a compressive modulus of about 3 MPa. This represents a six fold increase in compressive modulus. Similarly, the composite scaffolds also demonstrated a significantly higher tensile and shear moduli than that of the collagen scaffold.

Mineralization of collagen matrix increased the mechanical modulus of the scaffolds. The introduction of hydroxyapatite crystallites into the collagen fibrils restricted the deformation of the collagen fibril network. As a result, the viscous component of the collagen was reduced and elastic component was increased. This led to the decrease in tanδ value, as revealed by dynamic mechanical analysis (Fig. 7). It was observed that collagen scaffold has a tanδ value of 0.35 in compressive mode, which was reduced with the incorporation of hydroxyapatite and reached 0.1 for composite with a collagen/HAp ratio of 25/75. Similar effects were also observed for tensile and shear test modes.

4 Discussions

Bone is a dynamic tissue, subjected to a continuous renewing during the life of each individual by the process of bone remodelling. The coupling function of osteoclast and osteoblast can maintain a correct balance between bone resorption and osteogenic functions, thus maintaining a constant bone mass and strength[31]. In this process, the cells are assumed to provide "raw materials" and regulate the microenvironment for the formation of bone. It is generally believed that the osteoblasts release collagen molecules to form collagen fibrils. At the same time, calcium phosphate nanocrystals, provided by osteoblasts synthesize matrix vesicle, and epitaxially grow on collagen fibril to form strong hydroxyapatite-collagen nanocomposite.

The rationale for preparation of bone compositional mimic composite is to create a micro environment that more closely resembles the natural extra cellular matrix of the bone tissue. It is postulated that such environment would provide an appropriate micro-environment to support the cell growth and formation of new bone. In this paper, we have demonstrated that nano-hydroxyapatite could be incorporated into collagen fibrils by using a microwave-assisted *in situ* co-precipitation method. By introducing microwave during the precipitation process, the reaction between Ca^{2+} from calcium hydroxide and PO_4^{3-} from phosphoric acid could be accelerated significantly[32], and reduce the particle size also reported elsewhere[33].

By mixing a phosphorus acid-containing collagen solution with a calcium-containing solution, the two precipitations, i.e. collagen fibril formation and hydroxyapatite formation, were combined in one process step. In this way, both reactions were initiated simultaneously. When acid-containing collagen solution is titrated into the reaction vessel, which has a large quantity of deionized (DI) water with pH pre-adjusted to 8.5, the higher pH immediately induces collagen fibril formation. This was reflected by the rapid local turbidity increase as was observed during the experiment. These collagen fibrils are postulated to act as templates for the precipitation of hydroxyapatite crystallites. The collagen fibrils guide the precipitation of hydroxyapatite crystallites to form hydroxyapatite clusters deposit onto collagen fibrils directly, as revealed in TEM analysis (Fig. 5a).

Collagen fibrils are semi-crystalline aggregates of collagen molecules. Type-I collagen assembles its tropocollagen units in a quarter-staggered array, which leads to hole and overlap zones that can be seen as a periodic banding pattern[2]. These are actually bundles of fibrils that are assembled into a structure by regular spacing and rotation of molecules to produce a five stranded helical microfibrils which are axially staggered by multiples of units estimated at 66.8 nm[34]. In these staggered repeat of the microfibril, the part containing five molecules in cross-section is called as the "overlap" and the part containing only four molecules is called as the "gap". It is believed that when the collagen molecules are "soaked" in the phosphorous acid aqueous solution, some phosphate ions could enter into these "gaps". When the phosphorus acid-containing collagen solution contacts with a calcium-containing solution in the co-titration process, some calcium ions could diffuse into the collagen staggered gaps to react with phosphates ions that reside there to form apatite crystallites directly inside collagen fibres. In this way, homogeneously mineralised collagen fibrils could be obtained, as observed in TEM examination (Fig. 5b). The incorporation of nano-hydroxyapatite crystallites in the collagen fibrils restricts the strain deformation of collagen fibrils. This turns flexible collagen fibrils into more stiff fibrils, as

evidenced by the dynamic mechanical analysis shown in Fig. 7. The DMA analysis demonstrated that the collagen-hydroxyapate composites have significantly higher modulus and lower tanδ value than those of pure collagen scaffolds. The increase in stiffness can also be explained by the load transfer of the collagen to the higher modulus mineral component of the composite.

The molar ratio of calcium to phosphorus (Ca/P) of hydroxyapatite in this study was determined by the XPS analysis, and the elemental composition is listed in Table 1. The Ca/P molar ratio was calculated as 1.4, which was lower than the stoichiometric molar ratio of HAp at 1.67. However, a wide range of non-stoichiometry is allowed in the apatite system[35]. The calcium-deficient hydroxyapatite formation in this study may be attributed to the electrolysis of the orthophosphate ions.

For phosphorous acid, the conjugate base is the dihydrogen phosphate $H_2PO_4^-$, which in turn has a conjugate base of hydrogen phosphate HPO_4^{2-}. The hydrogen phosphate HPO_4^{2-} has a conjugate base of phosphate PO_4^{3-}. The dissolution of phosphoric acid is shown in the following reactions[36]:

$$H_3PO_4+H_2O=H_3O^++H_2PO_4^- \qquad K_{a1}=7.25\times10^{-3}, \quad (1)$$

$$H_2PO_4^-+H_2O=H_3O^++HPO_4^{2-} \qquad K_{a2}=6.31\times10^{-8}, \quad (2)$$

$$HPO_4^{2-}+H_2O=H_3O^++PO_4^{3-} \qquad K_{a3}=4.80\times10^{-13}, \quad (3)$$

where K_{a1}, K_{a2}, K_{a3} are acid dissociation constants given at 25°.

As a result of dissociation of phosphoric acid, its conjugate bases cover a wide pH range, and it is PH dependent. Thus the composition of an aqueous phosphorous acid is pH value dependant. From the equilibrium equation associated with the three reactions described above, for a 0.3 mM H_3PO_4 solution used in this study as starting material which has a pH of 3.30, the solution is mainly composed of $H_2PO_4^-$ with low concentration of HPO_4^{2-} and negligible PO_4^{3-}.

Since phosphate ions are absorbed to the collagen fibrils, they are less "mobile" than calcium ions. Therefore, the flux of phosphate ions is much lower than that of Ca^{2+} ions in the calcium-phosphate reaction system. The formation of apatite mainly depends on the diffusion of calcium ions. While calcium hydroxide is less soluble in water and the state of the phosphate ions depends on pH, the precipitation reaction involves the dissolution of calcium hydroxide, diffusion of the ionic species such as Ca^{2+} and hydroxide ions, and electrolysis of the orthophosphate ions. Although the pH in the bulk solution is maintained at 8.5 in this study by titrating of NaOH solution, the local pH value in the vicinity of phosphate ions may be lower than that of the bulk solution. Once non-stoichiometric crystals grow, it may take a longer time for the calcium ions to enter the lattice of the apatite to reach stoichiometric composition. This may explain the Ca-deficiency in the present of HAp. The formed hydroxyapatite is a defect apatite with small crystal size of about 30 nm. This gives the hydroxyapatite a lower crystallinity and higher solubility compared with stoichiometric hydroxyapatite and makes it similar to the apatite in the bone.

Table 1 Elemental composition of hydroxyapatite as determined by XPS analysis

Element	Position (eV)	FWHM	Area	Atom%*
O_{1s}	531.08	2.563	2437133	58.28
P_{2p}	347.08	2.432	1718084	23.99
Ca_{2p}	133.08	2.530	287636	17.11

* Ca/P =1.402

It worth mentioning that the collagen fibrils act as a template for nano-hydroxyapatite precipitation. The formation of collagen fibrils and their dispersion will determine the homogenicity of the nano-collagen/HAp composite. When the phosphorus acid-containing collagen solution contacts with a calcium-containing solution in the co-titration process, the formation of collagen fibrils occurs as a result of increase in local pH value. Simultaneously, nano-hydroxyapatites precipitate onto collagen fibrils to form nanocomposite granulates. These nano-granulates precipitate from the dispersion to the bottom of the reaction vessel. Even when the reactions are carried out under stirring, the local concentration and granulate size and shape may vary. As a result, the homogenicity across the whole sample may be compromised.

5 Conclusion

Collagen-hydroxyapatite composite scaffolds have been prepared by a microwave assisted *in situ* co-precipitation processing route. The method could combine the collagen fibril formation and hydroxyapatite formation in one process step, and both reactions were initiated simultaneously. The collagen fibrils formed are postulated to act as templates for the precipitation of hydroxyapatite crystallites during the co-precipitation process. There are two types of hy-

droxyapatite in the composite: interfibrillar apatite that precipitated onto collagen fibrils to form hydroxyapatite clusters, and intrafibrillar hydroxyapatite that precipitated directly inside collagen fibrils. The hydroxyapatite obtained in this study was a low crystalline calcium-deficient apatite with the molar ratio of calcium to phosphorus (Ca/P) of 1.4, which was lower than the stoichiometric molar ratio of 1.67. The mineralization of collagen matrix improved the mechanical properties of the scaffold significantly because the hydroxyapatite crystallites in collagen fibrils restricted the deformation of the collagen fibril network.

The method described could produce homogeneous bone-mimic collagen/HAp composite. However, to precisely control the precipitation and composition of hydroxyapatite inside collagen fibrils still a challenge, and is well worth further investigations.

Acknowledgment

The authors would like to acknowledge the support of Arthritis Research UK (Award 19429), the FP7 RESTORATION project (Award CP-TP 280575-2) and EPSRC MeDe Innivation (RGMECH103516).

References

[1] Zhou H, Lee J. Nanoscale hydroxyapatite particles for bone tissue engineering. *Acta Biomaterialia*, 2011, **7**, 2769–2781.

[2] Olszta M J, Cheng X G, Jee S S, Kumar R, Kim Y Y, Kaufman M J, Douglas E P, Gower L B. Bone structure and formation: A new perspective. *Materials Science and Engineering*: *R*: *Reports*, 2007, **58**, 77–116.

[3] Schmidt T, Stachon S, Mack A, Rohde M, Just L. Evaluation of a thin and mechanically stable collagen cell carrier. *Tissue Engineering*: *Part C*: *Methods*, 2011, **17**, 1161–1170.

[4] Lees S. Mineralization of type 1 collagen. *Biophysical Journal*, 2003, **85**, 204–207.

[5] Ficai A, Andronescu E, Voicu G, Ghitulica C, Vasile B S, Ficai D, Trandafir V. Self-assembled collagen/hydroxyapatite composite materials. *Chemical Engineering Journal*, 2010, **160**, 794–800.

[6] Wahl D A, Czernuszka J T. Collagen-hydroxyapatite composites for hard tissue repair. *European Cells and Materials*, 2006, **11**, 43–56.

[7] Freche M, Heughebaert J C. Calcium phosphate precipitation in the 60-80˚C range. *Journal of Crystal Growth*, 1989, **94**, 947–954.

[8] Lawson A C, Czernuszka J T. Collagen-calcium phosphate composites. *Proceedings of Institution of Mechanical Engineers*: *Part H*, 1998, **212**, 413–425.

[9] Langer R, Vacanti J P. Tissue engineering. *Science*, 1993, **260**, 920–927.

[10] Mastrogiacomo M, Scaglione S, Martinetti R, Dolcini L, Beltrame F, Cancedda R, Quarto R. Role of scaffold internal structure on in vivo bone formation in macroporous calcium phosphate bioceramics. *Biomaterials*, 2006, **27**, 3230–3237.

[11] Liu C Z, Czernuszka J T. Development of biodegradable scaffolds for tissue engineering: A perspective on emerging technology. *Materials Science and Technology*, 2007, **23**, 379–391.

[12] Sachlos E, Gotora D, Czernuszka J T. Collagen scaffolds reinforced with biomimetic composite nano-sized carbonate-substituted hydroxyapatite crystals and shaped by rapid prototyping to contain internal microchannels. *Tissue Engineering*, 2006, **12**, 2479–2487.

[13] Bradt J-H, Mertig M, Teresiak A, Pompe W. Biomimetic mineralization of collagen by combined fibril assembly and calcium phosphate formation. *Chemistry of Materials*, 1999, **11**, 2694–2701.

[14] Palmer L C, Newcomb C J, Kaltz S R, Spoeke E D, Stupp S I. Biomimetic systems for hydroxyapatite mimeralization inspired by bone and enamel. *Chemical Review*, 2008, **108**, 4754–4783.

[15] Liao S S, Cui F, Zhang W, Feng Q. Hierarchically biomimetic bone scaffold materials: Nano-HA/collagen/PLA composite. *Journal of Biomedical Materials Research Part B*: *Applied Biomaterials*, 2004, **69B**, 158–165.

[16] Suchanek W, Yoshimura M. Processing and properties of hydroxyapatite-based biomaterials for use as hard tissue replacement implants. *Journal of Materials Research*, 1998, **13**, 94–117.

[17] Kikuchi M, Ikoma T, Itoh S, Matsumoto H N, Koyama Y, Takakuda K, Shinomiya K, Tanaka J. Biomimetic synthesis of bone-like nanocomposites using the self-organization mechanism of hydroxyapatite and collagen. *Composites Science and Technology*, 2004, **64**, 819–825.

[18] O'Brien F J, Harley B A, Yannas I V, Gibson L J. The effect of pore size on cell adhesion in collagen-GAG scaffolds. *Biomaterials*, 2005, **26**, 433–441.

[19] Liu C, Xia Z, Czernuszka J T. Design and development of three-dimensional scaffolds for tissue engineering. *Chemical Engineering Research and Design*, 2007, **85**, 1051–1064.

[20] Liu C Z, Xia Z D, Han Z W, Hulley P A, Triffitt J T, Czernuszka J T. Novel 3D collagen scaffolds fabricated by indirect printing technique for tissue engineering. *Journal of*

Biomedical Materials Research B: *Applied Biomaterials*, 2008, **85**, 519–528.

[21] Yunoki S, Ikoma T, Monkawa A, Ohta K, Kikuchi M, Sotome S, Shinomiya K, Tanaka J. Control of pore structure and mechanical property in hydroxyapatite/collagen composite using unidirectional ice growth. *Materials Letters*, 2006, **60**, 999–1002.

[22] Sachlos E, Reis N, Ainsley C, Derby B, Czermuszka J T. Novel collagen scaffolds with predefined internal morphology made by solid freeform fabrication. *Biomaterials*, 2003, **24**, 1487–1497.

[23] Wahl D A, Sachlos E, Liu C Z, Czernuszka J T. Controlling the processing of collagen-hydroxyapatite scaffolds for bone tissue engineering. *Journal of Materials Science*: *Materials in Medicine*, 2007, **18**, 201–209.

[24] Feldkamp L A, Goldstein S A, Parfitt A M, Jesion G, Kleerekoper M. The direct examination of three dimensional bone architecture in vitro by computed tomography. *Journal of Bone and Mineral Research*, 1989, **4**, 3–11.

[25] Haddock S M, Debes J C, Nauman E A, Fong K E, Arramon Y P, Keaveny T M. Structure - function relationships for coralline hydroxyapatite bone substitute. *Journal of Biomedical Materials Research*, 1999, **47**, 71–78.

[26] Weiner S, Wagner H D. The material bone: Structure-mechanical function relations. *Annual Review of Materials Research*, 1998, **28**, 271–298.

[27] Liu C, Han Z, Czernuszka J T. Gradient collagen/nanohydroxyapatite composite scaffold: Development and characterization. *Acta Biomaterialia*, 2009, **5**, 661–669.

[28] Chang M C, Tanaka J. FT-IR study for hydroxyapatite/collagen nanocomposite cross-linked by glutataldehyde. *Biomaterials*, 2002, **23**, 4811–4818.

[29] Koutsopoulos S. Synthesis and characterization of hydroxyapatite crystals: A review study on the analytical methods. *Journal of Biomedical Materials Research*, 2002, **62**, 600–612.

[30] Müller F A, Müller L, Caillard D, Conforto E. Preferred growth orientation of biomimetic apatite crystals. *Journal of Crystal Growth*, 2007, **304**, 464–471.

[31] Kikuchi M, Itoh S, Ichinose S, Shinomiya K, Tanaka J. Self-organization mechanism in a bone-like hydroxyapatite/collagen nanocomposites synthesized in vitro and its biological reaction in vivo. *Biomaterials*, 2001, **22**, 1705–1711.

[32] Katsuki H, Furuta S. Microwave–versus conventional –hydrothermal synthesis of hydroxyapatite crystals from gypsum. *Journal of the American Ceramic Society*, 2004, **82**, 2257–2259.

[33] Vani R, Raja S B, Sridevi T S, Savithri K, Devaraj S N, Girija E K, Thamizhavel A, Kalkura S N. Surfactant free rapid synthesis of hydroxyapatite nanorods by a microwave irradiation method for the treatment of bone infection. *Nanotechnology*, 2011, **22**, 285701–285710.

[34] Piez KA, Miller A. The structure of collagen fibrils. *Journal of Supramolecular Structure*, 1974, **2**, 121–137.

[35] Osaka A, Miura Y, Takeuchi K, Asada M, Takahashi K. Calcium apatite prepared from calcium hydroxide and orthophosphoric acid. *Journal of Materials Science*: *Materials in Medicine*, 1991, **2**, 51–55.

[36] Margolis H C, Moreno E C. Kinetics of hydroxyapatite dissolution in acetic, lactic and phosphoric acid solutions. *Calcified Tissue International*, 1992, **50**, 137–143.